New Limits on the Electron Electric Dipole Moment from Cesium

S. A. Murthy, D. Krause, Jr., Z. L. Li,[a] and L. R. Hunter

Department of Physics, Amherst College, Amherst, Massachusetts 01002

(Received 23 January 1989; revised manuscript received 12 June 1989)

The electric dipole moment (EDM) of the ground state of cesium has been measured using a two-laser method that does not require the presence of an external **B** field. The measured value $d_{Cs} = (-1.8 \pm 6.7 \pm 1.8) \times 10^{-24}$ e cm implies that the electron EDM is $d_e = (-1.5 \pm 5.5 \pm 1.5) \times 10^{-26}$ e cm. This result represents more than an order-of-magnitude improvement over all previous limits.

PACS numbers: 35.10.Di, 11.30.Er, 32.80.Bx

Despite a search of more than twenty years, starting from the discovery of T (time reversal) violation in the K_0 meson system,[1] no further examples of T violation have been found. Some of the most sensitive searches have looked for a permanent electric dipole moment (EDM) of the neutron[2] or various atomic and molecular systems.[3] Three independent experiments on different atomic systems have all resulted in limits on the electron EDM of about 2×10^{-24} e cm.[4-6] Some gauge models predict that the electron EDM may be as large as 10^{-24} to 10^{-27} e cm.[7,8] We report new limits on the electron EDM based on a measurement of the EDM of cesium (d_{Cs}). Indeed, according to theory, a limit on the EDM of the cesium ground state results in a limit on the electron's EDM that is 120 ± 10 times smaller.[9-12]

We have developed a new two-laser scheme for measuring an atomic EDM in a cell that does not require the presence of any external **B** fields (except for calibration). The independence of the pump and probe beams permits separate optimizations of their intensities and frequencies, and more importantly, permits independent reversal of their helicities, resulting in a clear characterization of the various atomic polarizations.

Optical pumping is used to spin polarize (along x) the Cs ground state in the presence of an electric field **E** (along z). A term $-\mathbf{d}_{Cs} \cdot \mathbf{E}$ in the Hamiltonian would create a small precession of the polarization into the y direction. When the **E** field is reversed, the precession would be in the opposite sense. For small angles of rotation, the change in the component of the polarization along y when the applied **E** field is reversed is given by

$$\Delta P_y = 2P_x \omega_E \tau = 4P_x d_{Cs} E \tau / (2I+1) \hbar .$$

Here τ is the characteristic decay time of the polarization (≈ 15 ms), ω_E is the angular precession frequency in **E**, and $I = \frac{7}{2}$ is the nuclear spin. A measurement of a polarization along y that reverses with the applied **E** field is thus a measurement of d_{Cs}.

A schematic of the apparatus is shown in Fig. 1. The most critical elements in the apparatus are the cells that contain the Cs vapor. Each cell consists of a 1-cm-long, 1-in.-square segment of Corning 7052 glass tubing with tin-oxide–coated glass electrodes sealed onto the top and

bottom using Varian Torr-Seal epoxy. The cells are filled with 250 Torr of N_2 to minimize the Cs ground-state spin-relaxation rates. Two cells are stacked upon one another and $+4$ or -4 kV is applied to their common electrode while their outer electrodes are maintained at ground. The resulting electric fields in the two cells are opposed. By taking the difference between the precession signals observed in the two cells, the EDM signal is doubled while any precession associated with residual magnetic fields is canceled, to the extent that the residual **B** field is the same at the two cells.

The experimental cells are housed at the center of four large, cylindrical, high-permeability magnetic shields.
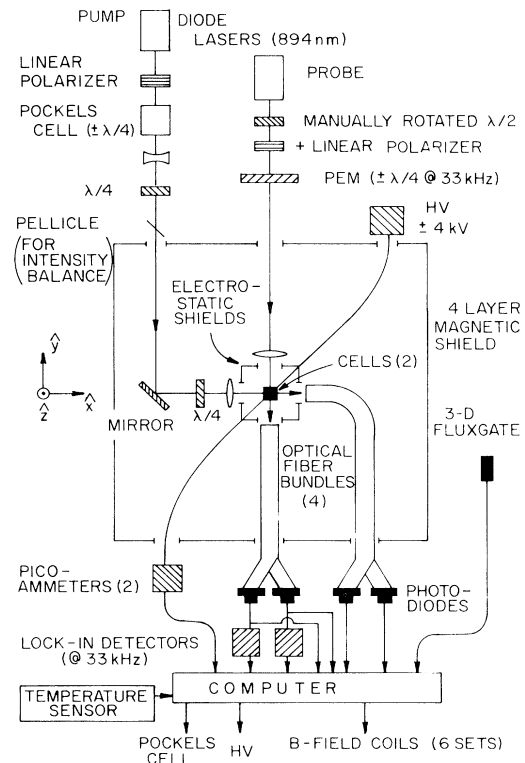

FIG. 1. Schematic diagram of the experimental apparatus (not to scale).

After degaussing, the shields reduce the residual field at the atoms to a few μG. The addition of a fluxgate-magnetometer–controlled feedback circuit to actively stabilize the longitudinal component of the magnetic field outside the shields results in an overall low-frequency dynamic shielding factor of about 3000 in all directions. Three orthogonal single-turn Helmholtz pairs and three sets of gradient coils supported within the shields are used to maintain all three components of the average magnetic field in each cell below 100 nG. These internal coils are under computer control, using the atoms themselves as the field sensors. These coils also produce a **B** field (~ 6 μG) along x which is reversed with the pump helicity and compensates for the Zeeman light shift[13] induced by the pump.

Optical pumping of the Cs ground state is accomplished by bathing the cells with circularly polarized 894-nm radiation (≈ 200 μW/cm^2) propagating along x. The light source is a single-mode 8-mW diode laser, tuned to the $6S_{1/2}, F = 3 \rightarrow 6P_{1/2}$ transition. The helicity of the light is determined by the polarity of the high voltage applied to a Pockels cell. Spin exchange and polarization transfer through the excited state result in a polarization of the $6S_{1/2}, F = 4$ state of approximately 70%. Upon inversion of the Pockels-cell polarity, the magnitude of the Cs ground-state orientation reverses to a precision of about 0.5%. A pair of optical fiber bundles transfer the pump light transmitted through the cells to detectors outside the magnetic shield to permit monitoring of the pump intensity and alignment.

The analysis of P_y is accomplished by probing the cesium cells with a much weaker (≈ 7 μW/cm^2) single-mode diode-laser beam, propagating along y and tuned to the $6S_{1/2}, F = 4 \rightarrow 6P_{1/2}$ transition. The circular polarization of the light is modulated at 33 kHz using a photoelastic modulator. An important feature of the modulated circular polarization is that the probe laser does no net pumping when averaged over a cycle. The probe beam light transmitted through the cells is transferred by optical fiber bundles to p-i-n silicon photodiodes outside of the magnetic shields. The transmission of the probe light for different helicities is $T_{\pm} = \exp[-k(1 \pm P_y)t]$, where k is the absorption coefficient, P_y is the y component of the ground-state polarization, and t is the cesium vapor's thickness. The value of kt is about 5% for our room-temperature cells. Synchronous detection of the photodiode output at the circular-polarization modulation frequency results in a signal whose amplitude is proportional to the component of polarization of the Cs ground state along y. Thus a change in the difference of the lock-in signals from the two cells when the **E** field is reversed constitutes a measurement of the EDM of the Cs ground state. To calibrate the measurement, we apply a 1.20-μG magnetic field first along z, then along $-z$, and observe the change in the lock-in signals due to the Hanle precession.

The data collection sequence begins with the nulling of the magnetic field at both cells and the calibration of each cell's sensitivity. A random-number generator then selects the electric field polarity and the helicity of the pump beam. After a 12-s wait to allow transient currents to die away, data acquisition begins. The integration is stopped after about 2 s and the pump helicity is then reversed. Following a 0.2-s wait, integration begins again. The pump helicity is reversed in this manner four times; then the applied E field is reversed and the sequence of helicity reversals is repeated. The E field is then turned off and the sequence is again repeated. The data are stored, and the appropriate sums and differences are calculated to extract the EDM signal and various diagnostic signals. This complete sequence requires about 70 s and constitutes a single data point. Ten such data points are collected, followed by two (or four) similar points taken in the presence of a known **B** field parallel and then antiparallel to y. These supplementary measurements are required in order to measure the quality of the electric field reversal. Following these measurements the **B** field is again zeroed, the sensitivity is again calibrated, and the entire sequence is begun again. After repeating this sequence three times, a set of diagnostic data that measure possible motional field effects is undertaken, ending the data collection cycle. This entire cycle requires about 1 h and is repeated about thirty times to complete a typical data set.

A linear polarizer and a half-wave plate before the photoelastic modulator are rotated every four cycles, changing the sign of all of the lock-in signals. An additional manual inversion of the high-voltage polarity to the field plates is also implemented every four data cycles, to insure that relay magnetic fields do not adversely affect the measurement. This reversal is staggered with respect to the linear polarization reversal.

Seven data sets were taken, yielding about 220 h of integration. The results are shown in Table I. Before each data set the cells are evacuated and the optics are realigned. The cell's orientations and positions were often changed between data sets. In addition, the magnetic field correction associated with the Zeeman light shift was removed in the third set. To eliminate data that may have been taken during a sudden change in the magnetic field or optics, all EDM points that exceed 3 standard deviations from the mean are removed from the data set (see Table I). The points rejected in this manner are most often associated with a sudden stress relaxation in the magnetic shields or experimental support structure.

Several possible sources of systematic error have been considered. The most important ones appear to be those associated with imperfect reversal of the electric field. The pseudoscalar that phenomenologically describes the observed T-violating interaction in our experiment is $\mathbf{J} \cdot (\mathbf{E} \times \boldsymbol{\sigma}) \tau$, where $\boldsymbol{\sigma}$ represents the initial atomic polar-

TABLE I. EDM data in units of 10^{-25} e cm. UC means uncorrected. 3σ indicates the data after truncating the points that deviate from the mean by more than 3 standard deviations; the uncertainties here have been multiplied by 1.015 to compensate for the artificial reduction in the standard error. In columns A and B the respective contributions from terms of the form $(\sigma \cdot J)E^2$ and $(\sigma \cdot E)(J \cdot E)$ have been sequentially removed. The cell's positions and orientations are as follows: S, standard; E, the cell's positions are exchanged; F, each cell has been flipped about the y axis.

Set	Cells	UC	3σ	A	B
1	E	-170 ± 146	-140 ± 144	-105 ± 145	-189 ± 161
2	S	-70 ± 133	-60 ± 133	-79 ± 133	-51 ± 136
3	S	-10 ± 200	-35 ± 202	-62 ± 203	-65 ± 206
4	S	70 ± 135	13 ± 128	47 ± 129	47 ± 129
5	S	-24 ± 241	25 ± 241	63 ± 245	57 ± 246
6	E,F	-98 ± 224	-75 ± 223	-14 ± 226	-12 ± 226
7	F	214 ± 279	288 ± 276	301 ± 276	307 ± 277
Avg.		-34 ± 65	-31 ± 64	-14 ± 65	-18 ± 67

ization, τ the spin relaxation time, and J the angular momentum of the analyzing photons. The signal is odd upon reversal of J, E, or σ. The small tensor polarizability of the Cs ground state (at 4 kV/cm the $m_F = 3$ and $m_F = 4$ sublevels of $F = 4$ are split by 0.2 Hz)[14] yields two scalar, T-conserving signals that in a similar way may be represented as $(\sigma \cdot E)(J \cdot E)$ and $(\sigma \cdot J)E^2$.

To the extent that E reverses precisely in magnitude and direction, these terms do not mimic the EDM signal. However, imperfections in the E reversal can result in a signal indistinguishable from the EDM. In an earlier measurement of the Stark shift of the Cs resonance lines, we studied the electric field reversal in cells and found that one cannot assume that the quality of the field reversal is the same as the quality of the voltage reversal.[15] In order to measure the quality of the E reversal during data acquisition we use another polarization, also due to the tensor polarizability of the Cs ground state, that has the form $(\sigma \cdot E)(\sigma \times E) \cdot J\tau$. This polarization is easily distinguished from the other polarizations because it does not reverse with the pump helicity. However, if the pump laser is tuned to the $D2$ line at 852 nm, effects associated with the large tensor polarizability of the $6P_{3/2}$ level become important. To avoid this complication we pump with the $D1$ line.

The application of a 22-μG magnetic field along y (B_y) precesses σ into the z direction, effectively increasing $\sigma \cdot E$ and enhancing both $(\sigma \cdot E)(J \cdot E)$ and $(\sigma \cdot E)(\sigma \times E) \cdot J\tau$. $J \cdot E$ and the relative size of E^2 for both cells and both polarities of the electric field may then be determined by observing the changes in the relevant polarizations with the reversal of B_y. In the last four data sets, supplementary measurements were also taken with $B_y = 8.8$ μG in order to have better sensitivity for the measurement of $J \cdot E$. Similarly, $\sigma \cdot E$ and $\sigma \cdot J$ may be deduced by examining the polarization $(\sigma \cdot E)(\sigma \times E) \cdot J\tau$ and $(\sigma \cdot J)E^2$ during normal data acquisition. This information may then be combined to

determine the total contribution to the EDM signal due to imperfect E reversal. A detailed description of this procedure will be described in a future paper. Typically, the imperfections in the electric field reversal are less than 1% of the mean field. After applying the appropriate corrections to remove these contributions from the EDM signals (see Table I) our result becomes $d_{Cs} = (-1.8 \pm 6.7 \pm 0.4) \times 10^{-24}$ e cm. The statistical uncertainties in our measurement of these contributions to the EDM have been combined in quadrature with the statistical uncertainty in the EDM itself. The second uncertainty is a conservative estimate of systematic uncertainty associated with these E field corrections. The sign is chosen such that for E parallel to B the splittings associated with E and B will have the same sign for negative d_{Cs}.

Another potential source of systematic error is associated with the leakage currents across the cells. If these currents circulate around the cell rather than flow directly across the cell, they could produce a magnetic field gradient that would reverse with the applied voltage and mimic our EDM signal. If the leakage current, which is typically less than 20 pA, were to circulate halfway around one cell, this would produce a false EDM signal of 1.4×10^{-24} e cm. We consider this to be a conservative upper limit on the possible contribution this effect might make. We add this systematic uncertainty linearly, yielding $d_{Cs} = (-1.86 \pm 6.7 \pm 1.8) \times 10^{-24}$ e cm. To illustrate the sensitivity of this measurement, we note that the statistical uncertainty here corresponds to a frequency splitting between adjacent magnetic sublevels in our cells of 1.6 μHz.

We also have considered possible systematic contributions to the EDM signal due to motional fields, Stark-induced interference, hyperfine mixing, misalignments, and polarization imperfections and find them to be unimportant at our present level of sensitivity. We have, in addition, performed extensive correlation tests between

the EDM and all other permutations of our signal, the three components of the ambient magnetic field, and temperature. No significant correlations are found.

Our limit on the cesium EDM results in a limit on the electron EDM of $d_e = (-1.5 \pm 5.5 \pm 1.5) \times 10^{-26} \, e$ cm. This represents more than an order-of-magnitude improvement over all previous measurements.[4-6]

Our result also places a limit on possible scalar-pseudoscalar T-violating electron-nucleon interactions of the form

$$H_s = C_s (G_F/2)(\bar{e} i \gamma_5 e) \bar{n} n \,,$$

where G_F is the Fermi coupling constant and e and n are the electron and nucleon operators. Our result combined with the calculation of Bouchiat[16] implies $C_s = (2.5 \pm 9.5 \pm 2.5) \times 10^{-6}$. This is now the best experimental limit on the coupling constant C_s.

Finally, we note that our result limits the size of the magnetic-quadrupole moment of the Cs nucleus,[17] $M_{Cs} = (3 \pm 13 \pm 3) \times 10^{-8} \mu_p r_{Cs}$, where $r_{Cs} = 6.1 \times 10^{-13}$ cm is the radius of the Cs^{133} nucleus and μ_p is the nuclear magneton.

The noise in our experiment associated with photon statistics is at least an order of magnitude smaller than our present experimental noise. With future improvements in our method of polarization measurement, laser beam stability, and magnetic shielding we hope to reduce significantly the experimental noise. New cell designs promise a reduction in the systematic effects associated with leakage currents and imperfect E reversal. We are thus hopeful that the next generation of this experiment will result in a significant improvement in our knowledge of possible T-nonconserving processes.

(a)On leave from the Institute of Physics, Academia Sinica, Beijing, China.

[1]J. H. Christenson, J. Cronin, V. L. Fitch, and R. Turlay, Phys. Rev. Lett. **13**, 138 (1964).

[2]V. M. Lobashev, in *Proceedings of the International Symposium on Weak and Electromagnetic Interactions in Nuclei, Heidelberg, West Germany, 1986*, edited by H. V. Klapdor (Springer-Verlag, Berlin, 1987), p. 866.

[3]For a review, see E. Hinds, in *Atomic Physics 11*, edited by S. Haroche, J. C. Gay, and G. Grynberg (World Scientific, Singapore, 1989).

[4]M. C. Weisskopf, J. P. Carrico, H. Gould, E. Lipworth, and T. S. Stein, Phys. Rev. Lett. **21**, 1645 (1968).

[5]M. A. Player and P. G. H. Sandars, J. Phys. B **3**, 1620 (1970).

[6]S. K. Lamoreaux, J. P. Jacobs, B. R. Heckel, F. J. Raab, and E. N. Fortson, Phys. Rev. Lett. **59**, 2275 (1987).

[7]M. B. Gavela and H. Georgi, Phys. Lett. **119B**, 141 (1982).

[8]A. Zee, Phys. Rev. Lett. **55**, 2382 (1985).

[9]P. G. H. Sandars, Phys. Lett. **22**, 290 (1966).

[10]W. R. Johnson, D. S. Guo, M. Idrees, and J. Sapirstein, Phys. Rev. A **32**, 2093 (1985); **34**, 1043 (1986).

[11]A. M. Martensson-Pendrill and Per Oster, Phys. Scr. **T36**, 444 (1987).

[12]B. P. Das, *Recent Advances in Many Body Theory* (Springer-Verlag, New York, 1988).

[13]B. S. Mathur, H. Tang, and W. Happer, Phys. Rev. **171**, 11 (1968).

[14]H. Gould, E. Lipworth, and M. C. Weisskopf, Phys. Rev. **188**, 24 (1969).

[15]L. R. Hunter, D. Krause, Jr., S. Murthy, and T. W. Sung, Phys. Rev. A **37**, 3283 (1988).

[16]C. Bouchiat, Phys. Lett. **57B**, 284 (1975).

[17]I. B. Khriplovich, Zh. Eksp. Teor. Fiz. **71**, 51 (1976) [Sov. Phys. JETP **44**, 25 (1976)].